

# Frequency scanning of a laser with a Littman–Metcalf cavity using an electrooptic deflector

S V Vasil'ev, L I Ivleva, V A Sychugov

**Abstract.** A new method for scanning a single-frequency laser with a Littman–Metcalf cavity using an electrooptic deflector is proposed and realised experimentally. The main advantages of such a scanning technique are its high precision and high frequency tuning rate, as well as the absence of mobile elements. It is shown that for a certain configuration of the cavity, the variation of the laser radiation wavelength can be synchronised with the optical length of the cavity, thus preventing mode hopping during scanning.

**Keywords:** frequency tuning, optical cavity, single-frequency laser.

## 1. Introduction

A promising cavity for narrow-band tunable lasers is a cavity in which a diffraction grating is mounted at a grazing incidence angle – the so-called Littman–Metcalf scheme or the GIG cavity [1, 2]. Fig.1 shows the schematic diagram of such a cavity. The cavity is formed by mirrors (1, 2) and a diffraction grating (3). The emission wavelength of a laser with the GIG cavity is determined by the relation

$$\lambda = A(\sin \theta + \sin \varphi), \quad (1)$$

where  $\lambda$  is the emission wavelength;  $A$  is the period of the diffraction grating;  $\theta$  is the angle of radiation incidence on the grating;  $\varphi$  is the diffraction angle. Laser scanning is carried out by rotating the mirror (2) (i.e., by varying the angle  $\varphi$ ). The radiation is usually outcoupled through the so-called specular order of the grating. The high dispersion of the grating provides a narrow-band or even a single-frequency lasing without using beam expanders or auxiliary intracavity frequency selectors.

Thus, the main advantage of lasers with the GIG cavity is the simplicity of their design. The minimum number of elements of the cavity simplifies the control of the laser and increases the stability of its characteristics. The drawback of the GIG cavity lasers is a comparatively low efficiency due to a low diffraction efficiency of the gratings at extremely small angles of incidence. Nevertheless, GIG cavity lasers

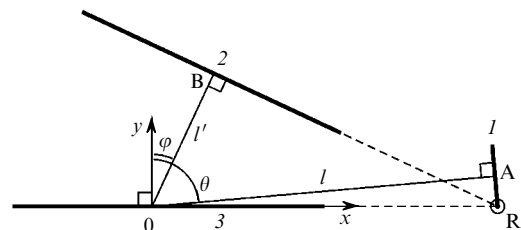


**Figure 1.** Schematic diagram of a GIG cavity preventing mode hopping during frequency scanning: (1, 2) mirrors, (3) diffraction grating, the symbol  $\square$  corresponds to a right angle.

have found quite wide applications. The aim of this paper is to realise an electrooptic scanning of a narrow-band laser with a Littman–Metcalf cavity, and to study its characteristics.

## 2. Application of an electrooptic deflector for scanning of a GIG cavity laser

A GIG cavity laser is normally tuned by rotating the mirror (2) (see Fig. 1). For a continuous scanning of a single-frequency laser, the variations in the lasing wavelength and the optical length of the cavity should be synchronised in such a way that mode hopping does not take place during scanning. The use of a GIG cavity allows a continuous scanning without complicating the laser design. If the GIG cavity is adjusted so that the planes of all cavity elements intersect along the same straight line passing through point R perpendicular to the cavity plane, and the rotation axis of the mirror (2) also coincides with this straight line, there will be no mode hopping during scanning (see Fig. 1) [3].

To verify this property of the GIG cavity, we put the origin of the Cartesian coordinates at the centre of the diffraction grating (3). Let  $l$  and  $l'$  be the lengths of the arms of the cavity. One can easily see that if the arm length  $l$  is fixed, then

$$\frac{l'}{l} = \frac{\sin \varphi}{\sin \theta}, \quad (2)$$

while the total length of the cavity is

$$L = l' + l = \frac{\sin \varphi + \sin \theta}{\sin \theta} l. \quad (3)$$

It follows from Eqns (1) and (2) that the longitudinal mode index is

$$q = \frac{2L}{\lambda} = \frac{2l}{\Lambda \sin \theta}. \quad (4)$$

This relation indicates that the longitudinal index does not depend on the diffraction angle  $\varphi$  and the lasing wavelength  $\lambda$ , and does not vary upon a rotation of the mirror (2).

The main problem encountered during a practical realisation of a continuous scanning of the laser is a high tuning rate  $\nu$ . The expression for the scanning rate can be derived easily from Eqn (1):

$$\frac{d\nu}{d\varphi} = -\frac{c}{\Lambda} \frac{\cos \varphi}{(\sin \varphi + \sin \theta)^2}, \quad (5)$$

where  $c$  is the velocity of light. Substituting the typical values of parameters for a GIG cavity ( $\theta \approx 89^\circ$ ;  $\varphi \approx 30^\circ$ ; and  $\lambda/\Lambda \approx 1.5$ ) into (5), we find that the scanning rate is approximately equal to  $10^4 \text{ GHz deg.}^{-1}$ . In other words, laser frequency tuning with an accuracy of about 100 MHz requires that mirror (2) must be fixed to within  $10^{-5}$  angl. deg. ( $0.05''$ ).

To solve this problem, the scanning of a GIG cavity laser by rotating a glass wedge placed between the mirror (2) and the grating (3) was proposed in Refs [4, 5]. A narrow wedge plays the role of an optical reducer which lowers the scanning rate by 2–3 orders of magnitude. Moreover, the theoretical study carried out in Ref. [6] showed that it is possible to avoid mode hopping during laser tuning by using a certain configuration of the GIG cavity with a reducer.

The introduction of an additional mobile element into the cavity considerably complicates the kinematic scheme and the laser adjustment procedure, thus nullifying all the advantages of using an optical reducer. In this connection, we propose the use of a wedge made of an electrooptic material (electrooptic deflector) for frequency tuning of a GIG cavity. In this case, the scanning is performed by changing the refractive index of the wedge instead of rotating it mechanically.

The schematic of a GIG cavity with an electrooptic deflector is shown in Fig. 2. The cavity consists of a mirror (1), a diffraction grating (3) and a deflector (4). The cavity mirror (2) is deposited on the back side of the deflector with the electrodes (5) deposited on its lateral surfaces. Rough tuning of the laser is performed by mechanically rotating the deflector (by changing the angle  $\beta$ ), while precise scanning is done by changing its refractive index  $n$ . If the planes of all cavity elements intersect along the same straight line passing through point R perpendicular to the cavity plane (Fig. 2), and the rotation axis of the deflector coincides with this straight line, there will be no mode hopping during precise as well as rough frequency scanning [6]. The proof of this property of the GIG cavity is analogous to the proof presented above for the 'standard' technique of laser scanning, but is more cumbersome and will not be given here.

The main advantages of the mechanism of precise scanning of the GIG cavity proposed here are the absence of mobile components and the extreme simplicity of the cavity. Rough tuning of the laser is accomplished by simply rotating the deflector, the self-consistent configuration of the cavity (which ensures that mode hopping does not take place) being preserved. It was shown in Ref. [6] that for a continuous scan of a laser in the range of several inverse centimetres, the precision of the deflector position tuning relative to mirror (1) and grating (3) must be a few tenths of a millimetre, which is quite acceptable.

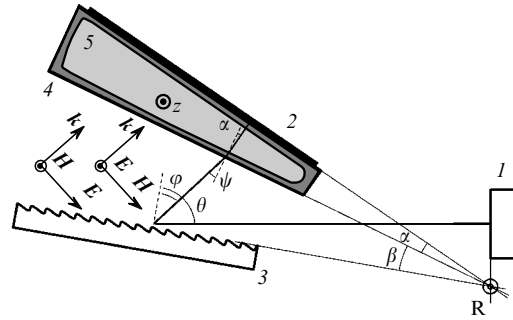


**Figure 2.** Schematic of a GIG cavity with an electrooptic deflector: (1, 2) mirrors; (3) diffraction grating; (4) electrooptic deflector; (5) electrodes across which the controlling voltage is applied;  $z$  is the optical axis of the crystal;  $\alpha$  is the refraction angle of the wedge;  $\beta$  is the angle between the deflector and the grating;  $\psi$  is the angle of incidence of radiation on the deflector.

Let us estimate the rate and range of the laser scan with the help of a deflector. From Eqn (5), we obtain

$$\frac{d\nu}{dn} = -\frac{c}{\Lambda} \frac{\cos \varphi}{(\sin \varphi + \sin \theta)^2} \frac{d\varphi}{dn}. \quad (6)$$

It follows from Fig. 2 that

$$\varphi = \psi + \beta \quad (7)$$

and

$$\sin \varphi = n \sin \alpha \cos \beta + \sqrt{1 - n^2 \sin^2 \alpha} \sin \beta. \quad (8)$$

Substituting (8) into (6), we arrive at the expression

$$\frac{d\nu}{dn} = -\frac{c}{\Lambda} \frac{\cos \varphi}{(\sin \varphi + \sin \theta)^2} \frac{\sin \alpha}{\sqrt{1 - n^2 \sin^2 \alpha}}. \quad (9)$$

Using the standard values of the parameters for the GIG cavity, we find that for the laser scan within the range of 300 GHz ( $10 \text{ cm}^{-1}$ ), the refractive index of the deflector should be changed by about 0.005, which is consistent with the characteristics of modern electrooptic crystals.

### 3. Investigation of the parameters of a laser with an SBN crystal deflector

Due to their high electrooptic coefficients and a broad transparency range, SBN ( $\text{Sr}_x\text{Ba}_{1-x}\text{Nb}_2\text{O}_6$ ) single crystals are among the most promising materials for the fabrication of efficient electrooptic deflectors [7].

SBN crystals belong to the symmetry class  $4mm$ . These are optically negative uniaxial crystals ( $n_o = 2.31$ ,  $n_e = 2.29$ ) having five nonzero tensor components of the electrooptic coefficients:

$$r_{13} = r_{23} \approx 7 \cdot 10^{-9} \text{ cm V}^{-1}, \quad r_{33} \approx 13 \cdot 10^{-8} \text{ cm V}^{-1}, \quad (10)$$

$$r_{42} = r_{51} \approx 4 \cdot 10^{-9} \text{ cm V}^{-1}.$$

If the electric field  $\mathbf{E}$  is directed along the optical axis  $z$ , the equation for the optical indicatrix of the crystal takes the form [8]

$$\left(\frac{1}{n_o^2} + r_{13}E_z\right)x^2 + \left(\frac{1}{n_o^2} + r_{13}E_z\right)y^2 + \left(\frac{1}{n_c^2} + r_{33}E_z\right)z^2 = 1. \quad (11)$$

Since  $r_{33} \gg r_{13}, r_{42}$ , the deflector efficiency will be the highest in the case when the radiation propagates perpendicular to the optical axis of the crystal and is polarised along this axis. Fig. 2 shows the arrangement of the deflector inside the cavity. The optical axis  $z$  of the crystal is perpendicular to the plane of the figure, and the solid arrows indicate the optimal directions of the electromagnetic field vectors  $\mathbf{k}$ ,  $\mathbf{E}$  and  $\mathbf{H}$ .

Eqn (11) gives the dependence of the refractive index of the deflector on the applied voltage. For the deflector configuration shown in Fig. 2, we obtain

$$n(U) = n_o \left(1 - \frac{r_{13}n_o^2}{2d}U\right) \text{ for TM polarisation wave,} \quad (12)$$

$$n(U) = n_c \left(1 - \frac{r_{33}n_c^2}{2d}U\right) \text{ for TE polarisation wave,}$$

where  $U$  is the applied voltage;  $d$  is the separation between the electrodes. Substituting expressions (12) into (9), we obtain the dependence of variation in the laser radiation frequency on the voltage across the deflector:

$$\delta\nu_{\text{TE}} = \frac{c}{A} \frac{\cos\varphi}{(\sin\varphi + \sin\theta)^2} \frac{\sin\alpha}{\sqrt{1 - n^2 \sin^2\alpha}} \frac{r_{33}n_c^2}{2d} \delta U, \quad (13)$$

$$\delta\nu_{\text{TM}} = \delta\nu_{\text{TE}} \frac{r_{13}n_o^3}{r_{33}n_c^3}.$$

For standard values of the cavity parameters and the values of the electrooptic coefficients given above for an SBN crystal, we obtain for  $d = 0.3$  cm

$$\frac{\delta\nu_{\text{TE}}}{\delta U} \approx 0.2 \text{ GHz V}^{-1}, \quad \frac{\delta\nu_{\text{TM}}}{\delta U} \approx 10.5 \text{ MHz V}^{-1}. \quad (14)$$

It follows from (14) that a change in the voltage by 500 V results in the laser tuning by 100 GHz ( $3 \text{ cm}^{-1}$ ) in the optimal case, which can be treated as a quite satisfactory result.

The experimental setup for verifying the operation of the electrooptic deflector was constructed on the basis of a single-frequency pulsed dye laser described in Ref. [9]. The laser was based on a GIG cavity with longitudinal pumping and the optical length of the cavity was 6 cm (the mode interval was 2.5 GHz). A copper vapour laser was for pumping, and the pumping radiation was transported to the active zone through a multimode fibre. The average pump power was 2 W for a pulse duration of 5 ns and a pulse repetition rate of 10 kHz. An alcohol solution of the RN-45 dye was used as the active medium.

Instead of the 'standard' mirror (2) (see Fig. 1) an electrooptic deflector (4) was placed in the cavity (see Fig. 2). The electrooptic deflector was made of an SBN crystal

grown by the method developed at the General Physics Institute, Russian Academy of Sciences [10]. The size of the deflector was  $16 \text{ mm} \times 3 \text{ mm} \times 4 \text{ mm}$ , and the prism angle was  $7^\circ$ . A multilayer dielectric mirror having the maximum reflectivity in the interval 550–600 nm was deposited on the back face of the prism, while an antireflection coating was applied on the front face. Graphite electrodes were deposited on the side faces of the prism. After coating, the crystal was transformed into a single-domain structure. A high-voltage power supply with a step adjustment of voltage in the interval 0.2–2 kV was used. A smooth variation of the voltage was possible in the interval of 200 V. The emission wavelength of the laser was measured with a LM01 wave-meter, and the output power was measured with an IMO-2N power meter.

The radiation resistance of the SBN crystal was measured before its use in the cavity. The experiments showed that the crystal could withstand a radiation load up to  $30 \text{ kW cm}^{-2}$  at 550–600 nm, which is several times higher than the values normally attained in a GIG cavity.

Fig. 3 shows the emission spectrum of a laser with an electrooptic deflector, obtained with the help of a Fizeau interferometer and a CCD array. One can see that the laser operates in the single-frequency mode, and the laser linewidth does not exceed 600 MHz (i.e., the width of the instrumental function of the interferometer). The average output power was 50–100 mW. Electronic scans of the laser frequency for a continuous and step regulation of the voltage are shown in Figs. 4 and 5, respectively. One can see that the tuning rate obtained with the help of an electrooptic scanning unit is about  $1 \text{ MHz V}^{-1}$ , the laser frequency depends linearly on the voltage across the deflector, and there is no hysteresis.

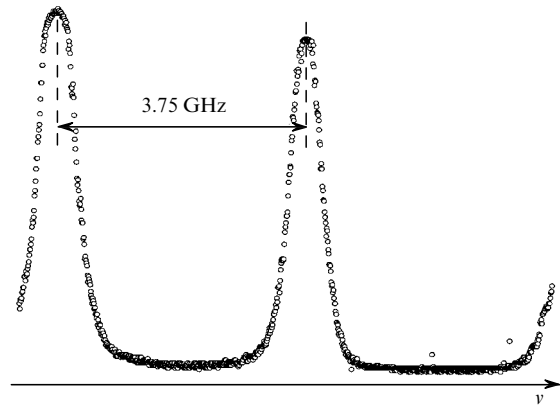
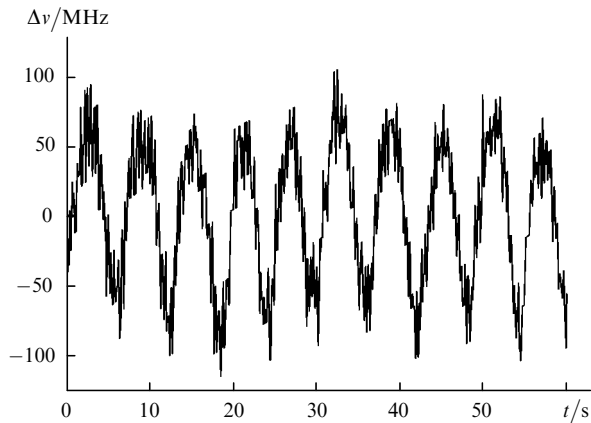
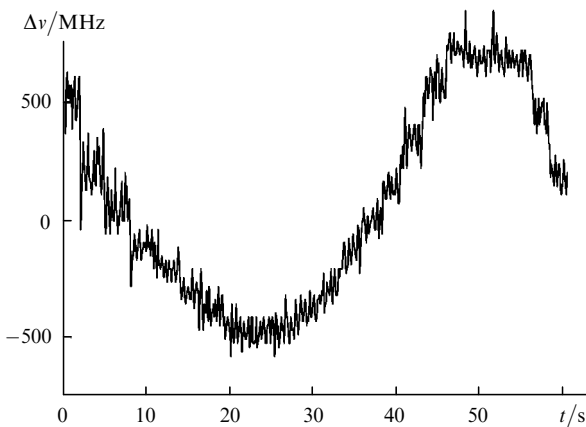


Figure 3. Emission spectrum of a dye laser.

The polarisation of radiation from a laser with a GIG cavity is determined by the properties of the diffraction grating. A standard diffraction grating with a metal coating was placed in the laser cavity. Such gratings have a high efficiency for TM polarisation and hence the laser radiation was TM-polarised, whereas the electrooptic effect in an SBN crystal is the strongest for the TE polarisation. The experimentally determined laser frequency scanning range differs noticeably from the theoretical one. We believe that such a difference is due to heating of the SBN crystal by laser radiation at 590 nm with an average power  $P_{\text{out}} \approx 0.1 \text{ W}$ , which induces depolarisation leading to a decrease in the electro-



**Figure 4.** Time dependence  $t$  of the detuning of the emission frequency  $\Delta\nu$  of a laser from its initial frequency  $\nu_0$  upon continuous variation of voltage in the interval  $U = 500 \pm 100$  V.



**Figure 5.** Time dependence  $t$  of the detuning of the emission frequency  $\Delta\nu$  of a laser from its initial frequency  $\nu_0$  upon stepwise variation of voltage in the interval from 200 to 1000 V.

optic coefficients of the crystal. Single SBN crystals are relaxation-type ferroelectrics with a blurred phase transition, which is manifested most clearly for SBN-75 ( $x = 0.75$ ) crystals at a temperature  $30\text{--}50^\circ\text{C}$ . For these crystals, the probability of depolarisation processes increases even upon a slight heating, which apparently occurred in our experiments.

Congruent SBN-61 crystals seem to offer greater prospects for future applications in electrooptic deflectors. The optical parameters of these crystals can be modified in each specific case by introducing dopants into them by retaining the high degree of optical homogeneity of the material.

**Acknowledgements.** The authors thank N M Polozkov and P A Lykov for their help in conducting the experiments. This work was supported by the programme 'Integration' (Grant No. A0103/99).

## References

1. Shoshan I, Danon N N, Oppenheim U P *J. Appl. Phys.* **48** 4495 (1977)
2. Littman M G, Metcalf H J *J. Appl. Opt.* **17** 2224 (1978)
3. Liu K, Littman M G *Opt. Lett.* **6** 117 (1981)
4. Greenhalgh D A, Sarkies P H *Appl. Opt.* **11** 895 (1982)
5. Kostritsa S A, Mishin V A *Kvantovaya Elektron.* **21** 502 (1994) [*Quantum Electron.* **24** 464 (1994)]
6. Vasil'ev S V, Kostritsa S A, Mishin V A *Zh. Tekh. Fiz.* **67** No. 3 53 (1997)
7. Prokhorov A M, Kuzminov Yu S *Ferroelectric Crystals for Laser Radiation Control* (Bristol: The Adam Hilger Series on Optics and Optoelectronics, 1991), p. 81
8. Mustel' E R, Parygin V N *Metody Modulyatsii i Skanirovaniya Sveta* (Methods for light modulation and scanning) (Moscow: Nauka, 1979), p. 73
9. Vasil'ev S V, Mishin V A, Shavrova T V *Kvantovaya Elektron.* **24** 131 (1997) [*Quantum Electron.* **27** 126 (1997)]
10. Ivlev L I, Bogodaev N V, Polozkov N M, Osiko V V *Opt. Mater.* **4** 168 (1995)
11. Vasil'ev S V, Sychugov V A *Kvantovaya Elektron.* **31** 72 (2001) [*Quantum Electron.* **31** 72 (2001)]